

# Driver Steering Model Based on a Target & Control Scheme

Han-Shue Tan, Jihua Huang, Fanping Bu, and Bakhtiar Litkouhi

**Abstract**—This paper aims to develop a driver steering model that can capture driver's key steering mechanisms from a control engineering point of view. Analyses with Double Lane Change (DLC) vehicle test data suggest that, instead of following the traditional concept of trajectory planning, drivers use target points located along the centerline of the lane they are changing to as references for control. The data also suggests that drivers engage steering rate control instead of steering angle control to steer the vehicle. Based on these analyses, this paper proposes a relatively straight-forward driver steering model based on this target & control scheme. Vehicle data of more than 80 DLC runs is used for the model verification. Both the open-loop identification and closed-loop simulations verify that this relatively simple driver steering model is capable of capturing driver's steering behavior and the simulated steering rate matches well with the actual steering rate.

## I. INTRODUCTION

Understanding and modeling drivers have attracted researchers from many disciplines such as cognitive science, control theory, psychology, and physiology for more than half a century. The topics involved are quite broad in scope. This paper relates to one of the control aspects of driving behavior: driver's steering control behavior.

As reviewed in [1-3], a large number of articles with driver models have been published. Some driver models are virtual driver models [4] designed to follow a prescribed route at a given or self-imposed speed by operating a virtual vehicle. They act like an automatic driving controller and capturing driver's driving behavior is not their emphasis. Some driver models do intend to capture driving behavior and typically try to match data from vehicle or driving simulator tests. For example, in [5], driver models are developed using neural networks (NN) to map the steering angle as a function of the time-delayed heading angle and lateral deviation from a desired trajectory. In [6], the steering controller is developed based on reinforcement learning. Hybrid driver models [7] and hierarchical driver models [8] are also typical in literature.

Despite those efforts, the full understanding of driving behavior still seem elusive. As claimed in [3], "to simulate a closed-loop ISO-lane change at the same maximum speed that an experienced human driver is able to perform is not

only a big, if not so far, but also an impossible challenge for a driver model." The commonly assumed elements of a driver steering model, such as trajectory planning and preview/prediction, seem to be reasonable, but they have not truly demonstrate their ability to capture driving behavior in various maneuvers yet.

As another attempt on this elusive topic, this paper aims to understand driver's steering behavior and to experimentally develop a driver steering model that can capture driver's key steering mechanisms from a control engineering point of view. To achieve this goal, the research has been conducted following two guidelines: (1) the commonly assumed or accepted elements in a driver model (e.g., trajectory planning and preview/prediction) are treated as hypotheses to be verified, and (2) the hypotheses and assumptions made are evaluated with vehicle test data, especially with steering angle and preferably steering rate. (Steering rate indicates driver's steering intents; therefore, it is important to capture the characteristics of the steering rate.) Ultimately, the model should be able to exhibit key characteristics of driver's steering behavior in closed-loop simulations.

As a starting point, a driver steering model for double lane change (DLC) maneuvers is developed and vehicle tests were conducted at a proving ground with 20 subject drivers to provide data of more than 80 test runs. Based on this data, this paper proposes and verifies a novel, relatively straight-forward driver steering model based on a target & control scheme. Instead of the traditionally assumed trajectory planning, the paper proposes that drivers do not plan and follow a desired trajectory during the DLC; instead, drivers use target points located along the centerline of the lane they are changing to as references for control. Accordingly, instead of predicting the deviations from the desired trajectory at the preview distance, the paper introduces target angle errors with respect to the target at the preview distance and proposes that the steering control is to regulate the target angle errors. Finally, unlike the typical steering angle control, the paper proposes a steering rate control based on the target angle errors following what the data have suggested.

Both open-loop analysis and closed-loop simulations are used to verify the proposed model. Not only does the simulated steering angle closely resemble the steering angle from vehicle tests, but the simulated steering rate also matches the steering rate from vehicle tests. Moreover, CarSim simulations with a verified nonlinear, complex vehicle model show that the relatively straight-forward model, when specifically tuned, can perform the DLC without hitting any cones at speeds as high as 105kph, which is higher than 85kph, approximately the highest speed a high-skilled driver can perform on the same DLC course.

Han-Shue Tan is with California PATH, University of California, Berkeley, CA 94804 (phone: (510) 665-3574, fax: 510-665-3537, email: hstan@path.berkeley.edu).

Jihua Huang is with California PATH, University of California, Berkeley, CA 94804 (email: jhuang@path.berkeley.edu).

Fanping Bu is with California PATH, University of California, Berkeley, CA 94804 (email: fanping@path.berkeley.edu).

Bakhtiar Litkouhi is with General Motors Global R&D and Planning, Warren, MI 48092 (email: bakhtiar.litkouhi@gm.com).

Preliminary control synthesis was conducted and several advantages of this driver steering model were revealed, including open-loop zeros with a constant damping at 0.707, which provides stability margin for drivers to increase their control gains when needed [10].

Although the development process involved multiple iterations, the paper describes the resultant model in a sequential fashion to make it easier to follow. The paper is organized as follows. Section II presents the proposed driver steering model. Section III introduces the DLC vehicle test data, and Section IV shows the model verification based on the DLC vehicle test data. Conclusions are provided in Section V.

## II. THE PROPOSED DRIVER STEERING MODEL

The driver steering model in this paper adopts a relatively broad scope as shown in Fig. 1. The inputs to the driver steering model include maneuver decisions (such as lane changes and left/right turns), road information, and vehicle motion information. The driver steering model then executes the desired maneuver based on the road information and the vehicle motion information.

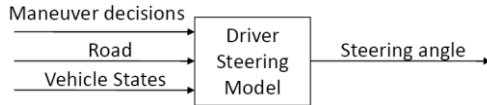


Fig. 1 Driver steering model

To understand and model driver's steering behavior, we start with understanding the steering behavior during DLC maneuvers. Compared to maneuvers such as lane keeping, (single) lane change and DLC maneuvers help induce trajectory planning behavior. Since DLC maneuvers are more demanding than lane changes, their data is likely to be richer and contains more distinct and definite characteristics.

The model development starts with examining the typical configuration of a driver steering model (Fig. 2), which includes three commonly assumed elements: trajectory planning (or path planning), preview/prediction, and steering control. The findings through these examinations form the foundation of the proposed driver steering model.

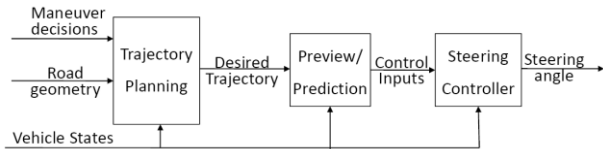


Fig. 2 Typical configuration of a driver steering model

### A. Trajectory Planning

It is generally assumed that drivers first plan a desired trajectory and then steer the vehicle to follow the desired trajectory. However, our closed-loop simulations with several assumptions<sup>1</sup> on the desired/planned path reveal that those assumptions cannot capture the non-linear, higher-frequency content in the steering angle (let alone the steering rate); that is, the simulated steering angle is typically much

<sup>1</sup> Such as an individual smooth trajectory derived based on the low-frequency content of the driver's actual trajectory, as well as a segment-by-segment polynomial curve that best fits the actual trajectory.

smoother than the actual steering angle in test data. Observations based on our own DLC test experiences lead to several hypotheses, which are then evaluated with the DLC vehicle test data. The data analysis suggests that, instead of planning and following a desired trajectory, drivers use target points as references for control and switch the target points based on the maneuver. Fig. 3 shows the proposed target points as control references during a DLC maneuver.

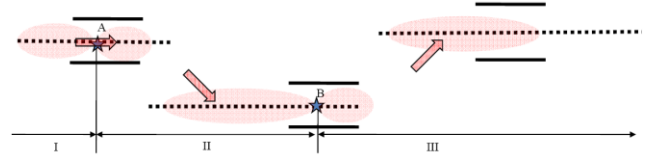


Fig. 3 Target sets (dotted line along the lane centerline)

The DLC course can be divided into 3 segments separated at the transition points A and B, the locations where a driver starts changing to the next lane. Therefore, A and B are also referred to as maneuver execution locations. Depending on the segment the current vehicle position is in, the corresponding moving target point is described below:

- Segment I (before Point A): the moving targets lie on the centerline of the lane defined by the first cone set;
- Segment II (between Point A and Point B): the moving targets lie on the centerline of the lane defined by the second cone set;
- Segment III (beyond Point B): the moving targets lie on the centerline of the lane defined by the third cone set.

The maneuver in Segment I is the lane keeping maneuver, and the moving targets are consistent with that of the traditional trajectory planning: the road itself. The maneuvers in Segments II and III are essentially lane changes (and the lane keeping afterwards); the moving targets represent the lanes the vehicle is changing to, which are quite different from the actual vehicle trajectory.

### B. Preview/Prediction

In literature, the preview/prediction module is included to mimic human's preview and predictive behavior. The preview behavior refers to that the human drivers perceive future path information within a finite future distance through visual cues. The prediction behavior assumes that the human drivers establish an internal vehicle dynamic model and predict vehicle's future trajectories [9].

In the proposed driver steering model, the traditional concept of preview/prediction still applies, but in a different fashion. At any specific time, the target point is a look-ahead distance (i.e., preview distance which may be varying) away from the vehicle position; therefore, it is also referred to as the preview target. Thus, given the maneuver execution locations A and B and a look-ahead distance  $d(t)$ , the preview target  $T(x_T(t), y_T(t))$  can be uniquely determined based on the current vehicle position  $(x(t), y(t))$ :

$$\left\| \begin{bmatrix} x_T(t) - x(t) \\ y_T(t) - y(t) \end{bmatrix} \right\| = d(t) \text{ and } \begin{bmatrix} x_T(t) \\ y_T(t) \end{bmatrix} \in \Pi, \quad (1)$$

Where  $\Pi$  is the centerline of the lane to which the vehicle is changing. In this DLC maneuver,  $\Pi$  is a function of the vehicle current position  $(x(t), y(t))$  and the maneuver

execution locations A and B. Figure 4 illustrates the preview targets for a few vehicle positions.

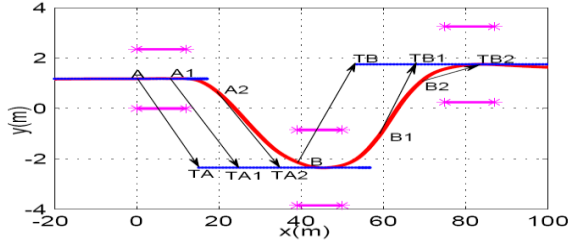


Fig. 4 Vehicle positions and the preview targets

Since the targets are fundamentally different from the “desired” trajectory, the traditional way of computing prediction errors as the future lateral deviations from the desired trajectory no longer applies. In the proposed driver steering model, the prediction is conducted based on the target heading angle as described below.

*Definition:* Target heading angle:

Given vehicle current position  $(x(t), y(t))$ , yaw rate  $\omega(t)$ , speed  $v(t)$ , and a target  $T(x_T(t), y_T(t))$ , and assuming the vehicle maintains its current yaw rate  $\omega(t)$  and speed  $v(t)$  (that is, the vehicle travels along a curve with a fixed radius  $R(t) = v(t)/\omega(t)$ ), the target heading angle  $\theta_d$  is the heading angle that ensures the vehicle will reach the target  $T$ .

Figure 5 illustrates the target heading angles,  $\theta_d$  and  $\theta_{d1}$ , corresponding to two targets  $T$  and  $T1$ , respectively. In Fig. 5(a), the vehicle maintains its current yaw rate  $\omega(t)$  and speed  $v(t)$ , while traveling towards the target point. Thus, the blue curvy lines are curves with the same fixed radius:  $R(t) = v(t)/\omega(t)$ . Figure 5(b) shows the special case where the current yaw rate is zero; the target heading angle is then determined by the straight lines connecting the target and the vehicle current position.

As illustrated in Fig. 6, the target heading angle can be computed as:

$$\theta_d = \beta + \gamma = \arctan\left(\frac{y_T(t) - y(t)}{x_T(t) - x(t)}\right) + \arcsin\left(\frac{d(t)}{2R(t)}\right) \quad (2)$$

where  $d(t)$  is the look-ahead distance (as in Eq. 1).

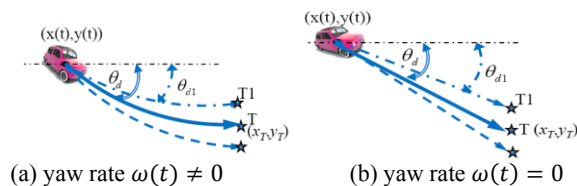


Fig. 5 Target heading angle

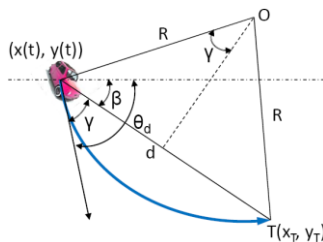


Fig. 6 Computation of the target heading angle

Therefore, we hypothesize that the target heading angle is the desired heading angle and the goal of the steering controller is to reduce the difference between the actual

vehicle heading angle and the target heading angle. Accordingly, we introduce the target angle error as the predicted error to be regulated by the steering controller:

$$\theta_e(t) = \theta_d(t) - \theta_v(t). \quad (3)$$

### C. Steering Controller

Accordingly, the input to the steering controller is the target angle error defined in Eq. 3 and the steering controller is to regulate the target angle error to zero. That is, the steering angle is a function of the target angle error:

$$\delta(t) = f(\theta_e(t)). \quad (4)$$

The structure of the control law is then chosen based on the relationship suggested by open-loop comparison, and the parameters of the controller are determined via open-loop identification (details in Section IV). The resulting control law is identified as a steering rate controller:

$$\dot{\delta}(t) = k(t)\theta_e(t) \quad (5)$$

While most steering controllers in driver models assume steering angle control rather than steering rate control, this control law implies that drivers do not have a desired steering angle as a control command to turn the steering wheel to. Instead, drivers determine how much and how fast changes in the steering angle are needed based on the target angle error and move the steering wheel to increase or reduce the steering angle according to the “desired” rates.

Eq. 5 shows the basic underlying steering controller; the actual steering control law will also include the time delay as well as the driver’s actuating “servo” characteristics of the driver due to driver physiologically limitations. That is:

$$\dot{\delta}(t) = g(\delta_{cmd}(t)) = g(k(t)\theta_e(t - \tau)) \quad (6)$$

The overall driver steering model is shown in Fig. 7. It follows a target & control scheme where target selection replaces the traditional trajectory planning and preview targets serves as references for a steering rate control<sup>2</sup>.

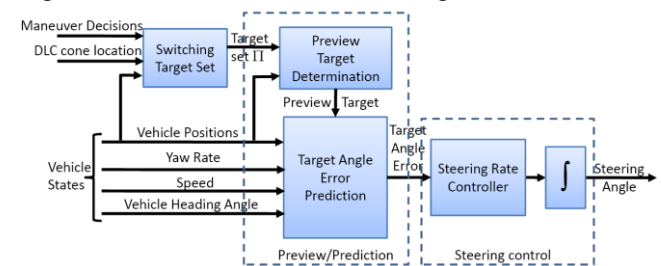


Fig. 7 The proposed driver steering model

### III. DLC VEHICLE TEST DATA

The model development and verification are based on DLC vehicle tests at a proving ground. Since the goal of this paper is to understand and model driver steering behavior in general rather than during limit handling conditions, the DLC tests are conducted on high-co surfaces and the data verifies that the vehicle is mostly in its linear region. The geometry of the DLC course (shown in Fig. 4) was derived from Draft International Standard ISO/DIS 3888-2

<sup>2</sup> Delays and driver “servo” will be present in the steering rate control. Perception errors will show up in both the prediction of the target angle error and the steering rate control. However, the details of these factors will not be included in this paper due to page limitations.

"Passenger cars- Test track for a severe lane-change maneuver" (i.e., the "Moose Test"). Traffic cones (shown as the magenta lines) were used to define the DLC course.

To ensure that the test data can capture both the common characteristics across drivers and the individuality of different drivers, twenty drivers of both genders and across a wide age range and different skill levels completed the tests. Each driver attempted the course at least four times, and a total of more than 80 DLC test runs were conducted.

A 4-door passenger vehicle was used and the data recorded include vehicle motion data (e.g., vehicle speed, yaw rate, lateral acceleration), driver's control input (including steering wheel angle, brake pedal position, throttle percentage), and vehicle positions (from a DGPS).

#### IV. MODEL VERIFICATION

The vehicle data of more than 80 DLC test runs is used for the model verification. Due to the page limitation, the results from two expert drivers of different driving style are shown here.

##### A. Target Selection & Preview/Prediction

The proposed target points as shown in Fig. 3 are verified together with the proposed preview/prediction based on the target heading angle. Figure 8 shows the configuration for the open-loop analysis with DLC vehicle test data.

For each DLC test run, the corresponding test data include the vehicle positions and heading angle from the DGPS, as well as the yaw rate, speed, and steering angle from on-board sensors. At any time instant  $t$ , the vehicle position  $(x(t), y(t))$ , together with the maneuver execution locations A and B, are used to first determine  $\mathcal{I}$ , the corresponding set of target points as shown in Fig. 3. The specific preview target at time  $t$ ,  $(x_T(t), y_T(t))$ , is then determined based on Eq. 1 once a look-ahead distance is given. Accordingly, the target heading angle  $\theta_d(t)$  is computed based on Eq. 2 using the yaw rate  $(\omega(t))$  and speed  $(v(t))$  from the test data. The target angle error is then computed with the target heading angle and the vehicle heading angle from the DGPS.

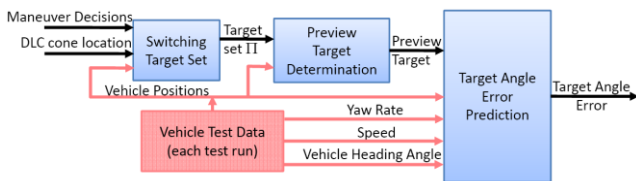


Fig. 8 Open-loop analysis based on DLC vehicle test data

Fig. 9 shows the target angle errors computed based on the vehicle test data from Subject #1's run #2. Four look-ahead distances are used for the computation: 15 m, 18 m, 21 m, and 24 m, and the corresponding target angle errors are shown as dashed lines in four colors: yellow, green, blue, and cyan. The maneuver execution locations A and B are assumed to be the starting location of the first and second cone sets, respectively<sup>3</sup>; therefore, there are sudden jumps in the target heading angle at the two maneuver decision

<sup>3</sup> The maneuver decision locations A and B will be identified based on each individual DLC test data in the subsequent controller identification.

locations. Both the steering angle and the normalized steering rate are plotted for comparison. The steering rate is computed by differentiating the steering angle measurements; it is further normalized with the mean speed of the corresponding test run for visual comparison purpose<sup>4</sup>.

As shown in Fig. 9, the target angle errors (shown as dashed lines) correlate quite well with the steering rate in the majority part (areas with shaded blue) of the lane changes. In particular, the target angle error at 21 m look-ahead distance (blue dashed line) yields the best correlation with the steering rate. This (open-loop) comparison suggests that the steering controller is likely a linear steering rate controller ( $\delta(t) = k(t)\theta_e(t)$  in Eq. 5) during most part of the DLC.

There are discrepancies between the target angle error and the steering rate at the beginning of the lane change. This is understandable since drivers are bounded in the steering acceleration; the steering rate has to increase continuously until it reaches the desired value as demanded by the target angle error. Once the steering rate meets the target angle error (at around the end of the first cone set for the first lane change and the end of the second cone set for the second lane change), the steering rate then follows the target angle error. From a control's perspective, this may indicate that the beginning of the lane change is conducted in a "catching-up" fashion, where the goal is to reach the desired value before regulation control starts. Using the same controller structure in Eq. 5 ( $\delta(t) = k(t)\theta_e(t)$ ), this phenomenon could suggest that the control gain  $(k(t))$  increases linearly at the beginning of the lane change and then more or less keeps constant for the remaining part of the lane change.

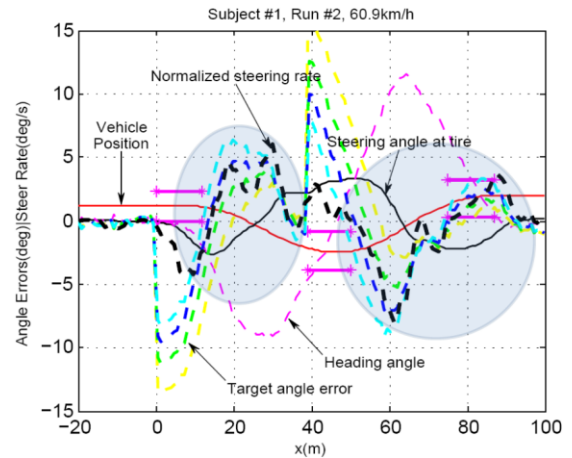


Fig. 9 Target angle error (Subject #1, Run #2)

The above observations hold true for all of the 80 test runs except the few cases where the subject drivers gave up completing the DLC course. Figure 10 shows the target angle errors computed based on the test data from Subject #2's run #2. Compared to Subject #1, Subject #2 engages more steering activities: the steering rate in Fig. 10 has larger maximum values and contains more high-frequency contents than the steering rate in Fig. 9. Subject #1 is

<sup>4</sup> The reason for the normalization is that the control gain  $k(t)$  in Eq. 5 increases as the vehicle speed increases. Therefore, the normalized steering rate shows a more consistent correlation with the target angle error than the steering rate itself. The normalization is for visual comparison purpose.

commonly referred to as a preview driver while Subject #2 is a feedback driver who is more like a race car driver. Despite the differences, the target angle error (at look-ahead distance between 18m (green) and 21m (blue)) captures the characteristics of the steering rate relatively well.

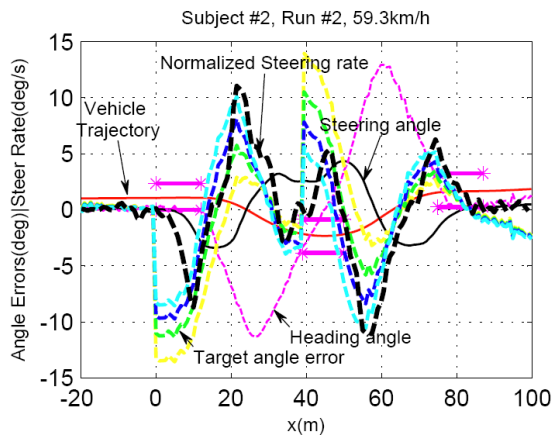


Fig. 10 Target angle error (Subject #2, Run #2)

### B. Controller Parameter Identification

The previous sub-section suggests that the steering control structure is a linear, steering rate control:  $\delta(t) = k(t)\theta_e(t)$ . As the target angle error can be computed based on the vehicle states, the steering control is uniquely defined if the controller gain ( $k(t)$ ) is identified. As shown in Eq. 6, the final steering controller also includes delays and driver “servo” characteristics, but for this initial model verification, the delay is estimated by data observation and the driver “servo” characteristics are ignored.

Therefore, using the computed target angle error and the steering rate from the same vehicle test run, the controller gain can be estimated. Since the controller gain can be time varying, the windowed least square estimation is used. Figure 11 shows the identified controller gains corresponding to Subject #1’s Run #3, with the look-ahead distances set to be 15m, 18m, 21m, and 24m. The vehicle trajectory, steering angle, and steering rate from the vehicle test data are also shown as reference. To make the plots easier to read, the trajectory is shifted down and the controller gain is scaled up by 2 and shifted upwards by 20.

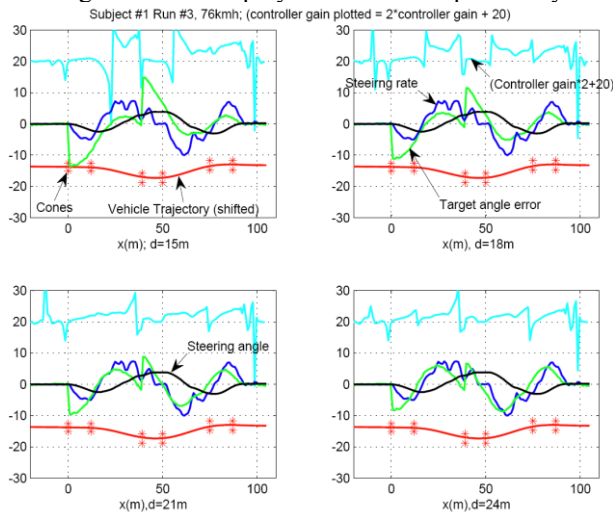


Fig. 11 Open-loop identified controller gains (Subject #1 Run #3)

Note that the identified controller gain becomes negative at locations where the steering rate crosses zero. This is mainly because the computation is sensitive around 0 (i.e., any slight mismatch or delay between the steering rate and the target angle error would generate relatively large changes in the control gain). Therefore, the identified controller gains at those locations are not trustworthy and typically the (steady state) values before or after the 0 crossing will be used in the closed-loop simulations.

### C. Closed-loop Simulations with the Open-Loop Identified Control Gains

Since the open-loop identification only suggests the possibility of a relationship, closed-loop simulation is used to verify the correctness and causality of the relationship. A bicycle model that has been verified against the vehicle test data is used in these simulations. Figure 12 shows the configuration of the closed-loop simulation. Unlike the open-loop analysis and identification in Fig. 8, the simulated vehicle states (rather than those from vehicle test data) are used to determine the target points, the target angle errors, and subsequently the steering angle (and rate command).

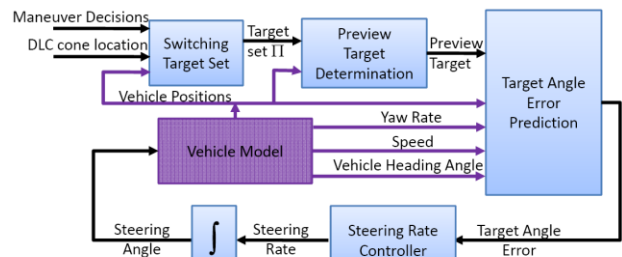


Fig. 12 Configuration for the closed-loop simulations

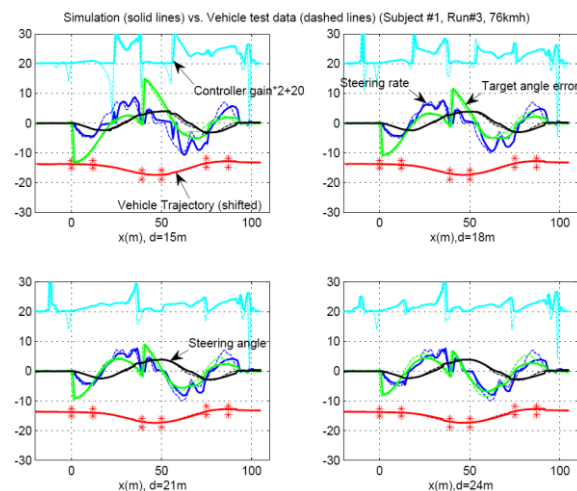


Fig. 13 Closed-loop simulation with controller gain based on the open-loop identification (Subject #1, Run 3)

Figure 13 shows the closed-loop simulation results with the modified controller gain. The modified gain is shown as the cyan solid line and the open-loop identified gain is shown as cyan dashed line. The simulation results are shown as solid lines while the vehicle test data is shown as dashed lines. Simulations with look-ahead distances of 18m and

21m match the actual steering rate well. The results of these closed-loop simulations are quite typical with data from other test runs. In short, these closed-loop simulations indicate that the simple steering rate control law is likely to be both correct and causal, and the proposed driver steering model can capture driver's steering behavior accurately.

#### D. Closed-loop Simulations with a Simplified Control Gain Structure

The control synthesis in [10] has shown that the resultant closed-loop system has two open-loop zeros at  $(-\frac{v}{a} \pm \frac{v}{a}i)$ . This rate controller is therefore likely to be able to sustain higher gains without sacrificing stability. It provides a reservoir of stability margin that allows the driver to increase his or her gain when higher gain is needed. Due to the page limitation, this paper will not get into the details of these analyses. The final controller has a simple control gain structure that includes a straight-forward gain scheduling mechanism to allow the control gain to increase by a couple of discrete steps based on some thresholds on the target angle error.

Fig. 14 shows the simulation results with this simple gain structure. Compared to the open-loop identified control gain (shown as the cyan dashed line), the control gain based on this simplified gain structure (shown as the cyan solid line) is straight-forward. The simulation results show that the proposed driver steering model with such a simple gain structure captures the driver's steering behavior adequately.

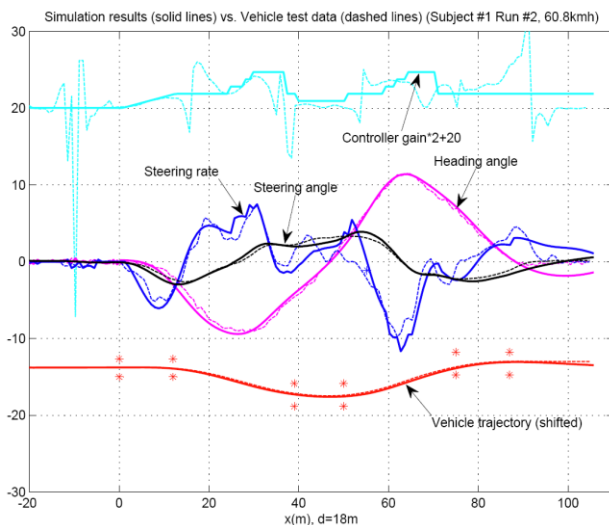


Fig. 14 Closed-loop simulation with the simplified controller gain structure (Compared to Subject #1 Run #2)

## V. CONCLUSION

This paper aims to understand driver's steering behavior and to develop a driver steering model that can capture driver's key steering mechanisms based on vehicle test data. The paper starts with examining the commonly assumed or accepted elements in a driver steering model. These elements include trajectory planning, preview/prediction, and steering controller. Our findings suggest that instead of planning and following a desired trajectory during the DLC, drivers seem to follow a target & control scheme for steering

control. That is, drivers use target points located along the centerline of the lane they are changing to as references for control. The vehicle test data also suggests that drivers predict target angle errors with respect to the preview targets and control the steering rate to execute the DLC maneuver.

Based on these findings, this paper develops a relatively straight-forward driver steering model based on the target and control scheme. Vehicle test data of 80 DLC runs is used for the model verification. The DLC vehicle test data shows consistent, good correlations between the steering rate and the target angle error. Furthermore, closed-loop simulations show that the relationship is likely to be correct and causal. The target-based steering rate control is further simplified and verified with simulations using both a bicycle model and a verified nonlinear, complex CarSim model<sup>5</sup>. The simulations show that the relatively simple driver steering model is capable of capturing driver's steering behavior and the simulated steering rate matches well with the actual steering rate.

## ACKNOWLEDGMENT

The authors would like to thank Drs Steve Chin, Bill Lin, Brian Repa, Kevin Deng, and Shih-Ken Chen of GM Global R&D and Planning for the valuable discussions and for their support.

## REFERENCES

- [1] T. Jürgensohn, *Hybride Fahrermodelle*. (Pro Universitate Verlag: Berlin) (ISBN 3-932490-22-3), (in German), 1997.
- [2] C.C. MacAdam, Understanding and modeling the human driver. *Vehicle System Dynamics*, 40(1-3), pp. 101-134, 2003.
- [3] M. Plochl and J. Edelmann, "Driver models in automobile dynamics application," *Vehicle System Dynamics*, vol. 45, pp. 699-741, 2007.
- [4] M. Irmscher, T. Jürgensohn, and H.-P. Willumeit, Driver models in vehicle development. *Vehicle System Dynamics Supplement*, 33, pp. 83-93, 1999.
- [5] K.F. Kraiss and H. Küttelwesch, "Teaching neural networks to guide a vehicle through an obstacle course by emulating a human teacher," *Proceedings of International Joint Conference on Neural Networks*, pp. 333-337, 1990.
- [6] Y. Koike and K. Doya, "Multiple state estimation reinforcement learning for driving model - driver model of automobile," *Proceedings of the IEEE Conference on Systems, Man, and Cybernetics*, Vol. 5, pp. 504-509, 1999.
- [7] T. Jürgensohn, T. Hybride Fahrermodelle. (Pro Universitate Verlag: Berlin) (ISBN 3-932490-22-3), (in German), 1997.
- [8] B. Cheng and T. Fujioka, "A hierarchical driver model," *Proceedings of IEEE Conference on Intelligent Transportation Systems*, pp. 960-965, 1997.
- [9] M. Vögel, O. von Stryk, R. Bulirsch, T.-M. Wolter, and C. Chucholowski, "An optimal control approach to real-time vehicle guidance," In: *Mathematics - Key Technology for the Future*, (Springer Verlag: Berlin), pp. 84-102, 2003.
- [10] J. Huang, H.-S. Tan, and F. Bu, "Preliminary studies in understanding a target & control based driver steering model," *American Control Conference*, San Francisco, CA, USA, June, 2011.

<sup>5</sup> Results of CarSim simulations are not included in this paper due to the page limitation.